

## Fusion calculations for $^{40}\text{Ca} + ^{40,44,48}\text{Ca}$

H. Esbensen, S. H. Fricke, and S. Landowne

*Physics Division, Argonne National Laboratory, Argonne, Illinois 60439*

(Received 19 June 1989)

Calculations are carried out for the  $^{40}\text{Ca} + ^{40,44,48}\text{Ca}$  fusion reactions, taking into account both the low-lying inelastic excitations and the dominant single-nucleon transfer reactions which couple directly to the entrance channels. The results agree well with the  $^{40}\text{Ca} + ^{40}\text{Ca}$  fusion data but they underpredict the low-energy  $^{40}\text{Ca} + ^{44,48}\text{Ca}$  measurements.

### I. INTRODUCTION

The study of how low-energy fusion rates depend on the structure of the colliding nuclei is an active area of research. A natural way to approach this problem theoretically is in terms of a coupled-channels formulation which explicitly includes the direct reaction processes. In this way, one calculates fusion as the difference between the total reaction cross section and that due to the direct reactions. The nuclear structure parameters in such fusion calculations are constrained by the experimentally observable direct reaction cross sections.

The coupled-channels approach is difficult to implement for heavy systems where many reactions are possible. It is also cumbersome to include nucleon transfer reactions in the traditional, microscopic way used in first-order perturbation calculations. Therefore, it is important to develop approximations to reduce the number of channels and also to simplify the treatment of transfer reactions.

A recent analysis of the  $^{58}\text{Ni} + ^{64}\text{Ni}$  fusion reaction used newly developed techniques to specifically study the effect of one-neutron transfer reactions.<sup>1</sup> It was found that after allowing for these transfer processes, in addition to the vibrational excitations, the calculations still underpredicted the low-energy fusion cross sections by a significant amount. Presumably, the discrepancy is due to the direct transfer of two nucleons.<sup>1</sup> A similar conclusion was reached for the case of  $^{28}\text{Si} + ^{64}\text{Ni}$  in Ref. 2.

In the present work we apply the techniques developed in Ref. 1 to study the fusion of calcium isotopes. It has been appreciated for some time that allowing for vibrational excitations is not sufficient to explain the variations that are observed in the  $^{40}\text{Ca} + ^{40,44,48}\text{Ca}$  fusion reactions.<sup>3,4</sup> A recent paper has reaffirmed this problem.<sup>5</sup> Another work has also estimated the effect of single-nucleon transfer for the  $^{40}\text{Ca} + ^{40}\text{Ca}$  system.<sup>6</sup> It is of particular interest, therefore, to explore the role which transfer reactions play in governing the low-energy fusion rates of the asymmetric combinations.

The following section briefly reviews the formulation for the coupled-channels calculations and the manner by which the single-particle transfer reactions and vibrational excitations are incorporated. The actual parameters which are used are then presented in Sec. III. The results

of the calculations are given in Sec. IV. Our conclusions are summarized in Sec. V.

### II. FORMALISM

#### A. Rotating frame approximation

To reduce the number of coupled channels we use the rotating frame approximation,<sup>7</sup> as was done in Ref. 1. This consists of transforming to a coordinate system where the  $z$  axis follows the projectile motion and then neglecting the Coriolis couplings that such a transformation generates. We only summarize the basic result here.

In the coupled-channels scheme, the radial wave functions are determined by solving the set of equations

$$\begin{aligned} \frac{\hbar^2}{2\mu_\beta} \left[ -\frac{d^2}{dr^2} + \frac{l_\beta(l_\beta+1)}{r^2} - k_\beta^2 \right] u_{\beta l_\beta}^J(r) \\ = - \sum_{\gamma l_\gamma I_\gamma} \langle \beta(l_\beta I_\beta) J | V | \gamma(l_\gamma I_\gamma) J \rangle u_{\gamma l_\gamma}^J(r), \end{aligned} \quad (2.1)$$

where  $J$  is the total angular momentum obtained by coupling the channel orbital angular momentum  $l_\beta$  to the total nuclear spin  $I_\beta$ . The channel energy is defined by

$$E + Q_\beta = \frac{\hbar^2 k_\beta^2}{2\mu_\beta}, \quad (2.2)$$

where  $E$  is the center-of-mass energy in the entrance channel,  $Q_\beta$  is the  $Q$  value for the reaction channel, and  $\mu_\beta$  is the corresponding reduced mass.

We shall only consider reactions which have spinless nuclei in the entrance channel. In that case, the rotating frame approximation is effectively introduced by replacing  $l_\beta$  on the left side of Eq. (2.1) with  $J$ . This amounts to ignoring terms of the order  $I_\beta/J$ . The equations to be solved in this approximation can then be reduced to

$$\begin{aligned} \frac{\hbar^2}{2\mu_\beta} \left[ -\frac{d^2}{dr^2} + \frac{J(J+1)}{r^2} - k_\beta^2 \right] u_{\beta I_\beta}^J(r) \\ = - \sum_{\gamma I_\gamma \lambda} F_{\beta I_\beta, \gamma I_\gamma}^\lambda u_{\gamma I_\gamma}^J(r), \end{aligned} \quad (2.3)$$

where the coupling element is

$$F_{\beta I_\beta, \gamma I_\gamma}^\lambda = (I_\gamma 0 \lambda 0 | I_\beta 0) \frac{1}{\hat{I}_\beta} \langle \beta I_\beta || V_\lambda || \gamma I_\gamma \rangle \frac{\hat{\lambda}}{\sqrt{4\pi}} \quad (2.4)$$

with  $\hat{I} \equiv \sqrt{2I+1}$ . The number of coupled channels has been reduced considerably. There is now only one channel for each physical state, characterized by its  $Q$  value and total nuclear spin,  $I_\beta$ . The coupled equations are solved with the boundary conditions of ingoing waves at a radius inside the barrier<sup>8</sup> in order to simulate the fusion process. They are matched in the usual way to appropriate Coulomb waves at a radius outside the range of the nuclear potential.

### B. Single-particle transfer

We treat the transfer of a single nucleon from a bound state of one nucleus with quantum numbers  $(l_1, \frac{1}{2}, j_1, m_1)$  to a bound state of another nucleus  $(l_2, \frac{1}{2}, j_2, m_2)$  in what is essentially a no-recoil approximation. The transfer interaction,  $V_{tr}$ , is taken to be the binding potential for one of the nuclei. Using wave functions of the form

$$\langle \mathbf{r}_i | l_i, \frac{1}{2}, j_i, m_i \rangle = \phi_{l_i}(r_i) [Y_{l_i}(\hat{\mathbf{r}}_i), \chi_{1/2}]_{j_i, m_i}, \quad (2.5)$$

the transfer matrix element can be written as

$$\begin{aligned} & \langle l_2, \frac{1}{2}, j_2, m_2 | V_{tr} | l_1, \frac{1}{2}, j_1, m_1 \rangle \\ &= \sum_{\lambda\mu} (j_1 m_1 \lambda \mu | j_2 m_2) \\ & \times \frac{1}{\hat{j}_2} \langle l_2 j_2 || V_{tr}^\lambda(r) || l_1 j_1 \rangle Y_{\lambda\mu}^*(\hat{\mathbf{r}}), \end{aligned} \quad (2.6)$$

where  $\mathbf{r}$  is the core-core separation. In the no-recoil approximation we have

$$\mathbf{r}_1 = \mathbf{r} + \mathbf{r}_2. \quad (2.7)$$

A mass-dependent factor of

$$\left[ \frac{4m_a m_b}{(m_a + m_b)(m_A + m_B)} \right]^3 \quad (2.8)$$

is included in the actual calculation of the matrix elements to partially account for recoil effects.<sup>9</sup>

In Ref. 1, the transfer matrix elements were calculated using an analytic approximation based on the Buttler-Goldfarb method.<sup>9</sup> In the present work we evaluate the matrix elements directly by using numerical wave functions for each of the single-particle states. A straightforward method of rendering the matrix element into the form of Eq. (2.6) is to use the Fourier transforms of the wave functions.<sup>10</sup> The result is

$$\begin{aligned} & \frac{1}{\hat{j}_2} \langle l_2 j_2 || V_{tr}^\lambda(r) || l_1 j_1 \rangle = (-1)^{j_1 + j_2 + \lambda + l_1} \\ & \times \frac{4}{\sqrt{\pi}} \frac{\hat{j}_1 \hat{\lambda}}{\hat{j}_2} (j_1 \lambda \frac{1}{2} 0 | j_2 \frac{1}{2}) \\ & \times A_\lambda(r), \end{aligned} \quad (2.9)$$

where

$$A_\lambda(r) = \int_0^\infty dq q^2 j_\lambda(qr) \tilde{\phi}_{l_2}(q) \tilde{F}_{l_1}(q) \quad (2.10)$$

and

$$\tilde{\phi}_l(q) = \int_0^\infty dr r^2 \phi_l(r) j_l(qr) \quad (2.11)$$

$$\tilde{F}_l(q) = \int_0^\infty dr r^2 \phi_l(r) V_{tr}(r) j_l(qr). \quad (2.12)$$

In these equations,  $j_l(x)$  is the spherical Bessel function. In deriving Eq. (2.10), the binding potential for the donor nucleus has been used for the transfer potential. Using the potential of the recipient nucleus would involve an obvious modification to these equations.

We also make use of an additional approximation to reduce the number of transfer channels in the coupled equations. The total intrinsic spin  $\lambda$  for a given nucleon transfer between a specific pair of single-particle states can have several different values. Each one is associated with an independent transfer channel  $\beta$  which has a coupling  $F_{\beta\lambda, \alpha 0}^\lambda$  with the spinless entrance channel  $\alpha$ . These transfer channels all have the same  $Q$  value. In the actual calculations we replace them by a single effective channel with a coupling strength defined by

$$F_{\beta, \alpha} \equiv \left[ \sum_\lambda |F_{\beta\lambda, \alpha 0}^\lambda|^2 \right]^{1/2}. \quad (2.13)$$

This effective coupling for each set of single-particle states was found to work very well in Ref. 1. It is usually dominated by the contribution which has the largest total intrinsic spin.

### C. Vibrational couplings

The couplings to surface vibrations are treated in a standard fashion.<sup>11</sup> We only include first-order vibrational excitations in the initial mass partition. The second-order excitation processes which were found to be important for the Ni + Ni system in Ref. 11 are weaker in the Ca + Ca case because the strength of the coupling interactions in the barrier region decreases for lighter mass systems and also the excitation energies increase. The minor effect of the second-order couplings in the present case will be shown explicitly in Sec. IV. The relevant single phonon couplings are given by

$$\begin{aligned} \langle \lambda || V_{cpl}^\lambda(r) || 0 \rangle &= -\sigma_n \frac{dU}{dr} \\ &+ \sigma_c \frac{Z_1 Z_2 e^2}{r^2} \frac{3}{2\lambda + 1} \left[ \frac{R_c}{r} \right]^{\lambda - 1}, \end{aligned} \quad (2.14)$$

where  $\lambda$  is the multipolarity of the excited vibration,  $\sigma_n$  and  $\sigma_c$  are the nuclear and Coulomb coupling strengths, and  $U(r)$  is the nuclear ion-ion potential. The coupling strengths are given in terms of the deformation lengths by

$$\sigma_i = \frac{\delta_i}{\sqrt{4\pi}}. \quad (2.15)$$

A complete calculation must include excitations in both the projectile and target nuclei. In this work we

reduce the number of inelastic channels by introducing an approximation that combines target and projectile excitations of identical multipolarity into a single effective vibration. The effective coupling strengths and excitation energies for this effective vibrational channel are defined in terms of the original strengths and energies by

$$\sigma' = \left[ \sum_i \sigma_i^2 \right]^{1/2} \quad (2.16)$$

and

$$E' = \sum_i \sigma_{n_i}^2 E_i / \sum_i \sigma_{n_i}^2. \quad (2.17)$$

This projectile-target symmetrization is obviously exact for a reaction involving identical nuclei.

### III. PARAMETERS

Since the absorption of flux out of the elastic channel is introduced through the effects of coupling to the other channels and by the ingoing wave boundary conditions, the ion-ion potential representing the interaction between the nuclei is purely real. We take this potential to have a Woods-Saxon shape essentially as determined in Ref. 12. The diffusivity is  $a=0.63$  fm and the depth is determined by

$$V_o = -31.67 \frac{R(A_1)R(A_2)}{R(A_1)+R(A_2)} \text{ MeV}, \quad (3.1)$$

where the nuclear radii are given by

$$R(A) = (1.233 A^{1/3} - 0.98 A^{-1/3}) \text{ fm}. \quad (3.2)$$

The potential radius of Ref. 12 is given by

$$R(A_1, A_2) = R(A_1) + R(A_2) + 0.29 \text{ fm}. \quad (3.3)$$

Because we are concentrating on the variation in the structure of the calcium isotopes, we have used a different construction for the potential radius, namely,

$$R(40, A_2) = R(40) + R(40) \frac{R_{\text{rms}}(A_2)}{R_{\text{rms}}(40)} + \Delta, \quad (3.4)$$

where  $R_{\text{rms}}(A)$  are the root-mean-squared matter radii for the calcium isotopes given in Ref. 13. A fit of the no-coupling calculations to the fusion data for  $^{40}\text{Ca} + ^{40}\text{Ca}$  at energies above the barrier was made to determine  $\Delta=0.21$  fm. This value is well defined since, according to the forthcoming calculations, the couplings have little effect on the  $^{40}\text{Ca} + ^{40}\text{Ca}$  fusion cross sections above the barrier. The potential parameters for the three cases

TABLE I. The ion-ion potential parameters used in the calculation. Also shown are the heights and positions of the resulting Coulomb barriers.

	$V_o$ (MeV)	$R$ (fm)	$V_{\text{bar}}$ (MeV)	$R_{\text{bar}}$ (fm)
$^{40}\text{Ca} + ^{40}\text{Ca}$	62.235	8.070	55.03	9.742
$^{40}\text{Ca} + ^{44}\text{Ca}$	63.363	8.173	54.35	9.877
$^{40}\text{Ca} + ^{48}\text{Ca}$	64.384	8.207	54.08	9.931

TABLE II. The Coulomb and nuclear coupling strengths ( $\sigma_c$  and  $\sigma_n$ ) and excitation energies  $E^*$  for the low-lying vibrational states in the Ca isotopes. The nuclear strengths were obtained from analyzing  $^{16}\text{O}$  inelastic scattering data in Refs. 14 and 15.

	$\lambda$	$\sigma_c$ (fm)	$\sigma_n$ (fm)	$E^*$ (MeV)
$^{40}\text{Ca}$	$3^-$	0.4650	0.3150	3.737
	$2^+$	0.1380	0.1250	3.905
	$5^-$	0.3420	0.1750	4.492
$^{44}\text{Ca}$	$2^+$	0.3047	0.2398	1.157
	$4^+$	0.1495	0.0818	2.283
	$2^+$	0.1044	0.0903	2.656
	$4^+$	0.0451	0.0423	3.044
	$3^-$	0.2454	0.1693	3.308
$^{48}\text{Ca}$	$5^-$	0.1326	0.0931	3.914
	$2^+$	0.1260	0.1900	3.832
	$3^-$	0.2500	0.1900	4.505
	$5^-$	0.0490	0.0380	5.146

along with the resulting barrier heights and radii are given in Table I.

The coupling strengths for the excitation of the different Ca isotopes are listed in Table II. These values are either equal to or somewhat modified from the strengths obtained by analyzing  $^{16}\text{O}$  inelastic scattering in Ref. 14. The modified values were found to reproduce the scattering of  $^{16}\text{O}$  on  $^{40}\text{Ca}$  and  $^{48}\text{Ca}$  in a recent coupled-channels analysis which uses a purely real potential with the same scaling procedure as before.<sup>15</sup> The effective excitations and strengths used in the actual calculations, obtained as described in the preceding section, are given in Table III. For the  $^{40}\text{Ca} + ^{44}\text{Ca}$  case, the  $2^+$  projectile and target states are included exactly since their energies are too different for the symmetrization procedure to be accurate.

The ground-state  $Q$  values for various transfer reac-

TABLE III. The effective Coulomb and nuclear coupling strengths and the effective excitation energies for the vibrational channels used in the calculations. These are obtained from the values in Table II using the prescription given in Eqs. (2.16) and (2.17).

	$\lambda$	$\sigma'_c$ (fm)	$\sigma'_n$ (fm)	$E'$ (MeV)
$^{40}\text{Ca} + ^{40}\text{Ca}$	$3^-$	0.6576	0.4455	3.737
	$2^+$	0.1952	0.1768	3.905
	$5^-$	0.4837	0.2475	4.492
$^{40}\text{Ca} + ^{44}\text{Ca}$	$2^+$	0.3047	0.2398	1.157
	$4^+$	0.1562	0.0921	2.444
	$2^+$	0.1044	0.0903	2.656
	$3^-$	0.5258	0.3576	3.643
	$2^+$	0.1380	0.1250	3.905
$^{40}\text{Ca} + ^{48}\text{Ca}$	$5^-$	0.3668	0.1982	4.363
	$2^+$	0.1869	0.2274	3.853
	$3^-$	0.5279	0.3679	3.944
	$5^-$	0.3455	0.1791	4.520

TABLE IV. Ground-state  $Q$  values for various transfer reactions.

		$Q$ (MeV)				
		$1n$	$1p$	$2n$	$2p$	$\alpha$
$^{40}\text{Ca} + ^{40}\text{Ca}$	Pickup	-7.27	-7.24	-9.1	-9.86	-1.92
	Stripping	-7.27	-7.24	-9.1	-9.86	-1.92
$^{40}\text{Ca} + ^{44}\text{Ca}$	Pickup	-2.77	-11.1	0.774	-16.8	-3.72
	Stripping	-8.22	-1.44	-11.1	2.53	2.41
$^{40}\text{Ca} + ^{48}\text{Ca}$	Pickup	-1.59	-14.7	2.62	-24.2	-9.25
	Stripping	-10.5	1.29	-17.4	7.08	0.637

tions are given in Table IV. For the  $^{40}\text{Ca} + ^{44,48}\text{Ca}$  cases, the  $Q$  values for single proton pickup and neutron stripping are large and negative. These channels are ignored. The final states for the single-nucleon transfers which are actually included in the calculations are collected in Tables V–VII, together with the relevant spectroscopic factors. For the symmetric system  $^{40}\text{Ca} + ^{40}\text{Ca}$ , the pickup reactions are identical to the stripping reactions, so including only one type and multiplying the matrix element by  $\sqrt{2}$  accounts for both processes. In all of the calculations we have used the nuclear binding potential of the  $^{40}\text{Ca}$  projectile as the transfer potential. It should be noted in Table IV that there are well-matched channels available for two-particle and alpha-particle transfer reactions. Some speculations on the possible influence of these processes will be given in the following section.

#### IV. CALCULATIONS

The fusion cross sections obtained when only vibrational excitations are included are shown in Fig. 1. In each case, the subbarrier cross sections are significantly larger than those obtained from a no-coupling calculation. These enhancements generally agree with those obtained in Ref. 4 using a matrix diagonalization approximation and with recent calculations<sup>5</sup> where the effects of vibrational excitations were included through an effective polarization potential. As shown by the dashed curves in Fig. 1, including second-order vibrational effects<sup>11</sup> only

TABLE V. Particle and hole states generated in one-neutron and one-proton pickup or stripping reactions on  $^{40}\text{Ca}$ . The excitation energies, spins and parities, and spectroscopic factors are given for the different states of the final nucleus. The spectroscopic factors for  $^{39}\text{Ca}$ ,  $^{41}\text{Ca}$ ,  $^{39}\text{K}$ , and  $^{41}\text{Sc}$  are from Refs. 16–19, respectively.

$^{40}\text{Ca}$	$J^\pi$	$E$ (MeV)	$C^2S$
$^{39}\text{Ca}$	$\frac{3}{2}^+$	0.00	3.70
$^{41}\text{Ca}$	$\frac{7}{2}^-$	0.00	0.95
	$\frac{3}{2}^-$	1.94	0.70
$^{39}\text{K}$	$\frac{3}{2}^+$	0.00	4.23
	$\frac{1}{2}^+$	2.52	1.62
$^{41}\text{Sc}$	$\frac{7}{2}^-$	0.00	1.12

slightly increases the fusion cross sections over the first-order results. These effects will not be included in the calculations which follow. It is clear that vibrational excitations alone cannot account for the subbarrier fusion cross sections for the  $^{40}\text{Ca} + ^{44,48}\text{Ca}$  cases. It should also be noted in these cases that the no-coupling calculations slightly overpredict the cross sections at energies above the barrier. The potential radii could be reduced to achieve agreement with these higher-energy data points. This would cause a corresponding decrease in the calculated subbarrier cross sections, thereby increasing the discrepancy with the lower-energy data.

The results of the calculations where both vibrational excitations and single-nucleon transfer channels are included are shown by the solid curves in Fig. 2. Also shown by the dashed curves are the results obtained when only the transfer channels are included. A comparison of Fig. 2 with Fig. 1 shows that the enhancement obtained due to transfer alone is similar in magnitude to that obtained with vibrational excitations. However, the combined effect is not a simple addition of the two. Figure 2 shows that the full calculation for  $^{40}\text{Ca} + ^{40}\text{Ca}$  agrees rather well with the data (see also Ref. 6). For instance, the small discrepancy could be attributed to the higher-order vibrational couplings (see Fig. 1). However, the subbarrier fusion cross sections in the  $^{40}\text{Ca} + ^{44,48}\text{Ca}$  cases remain well below the data when the single-nucleon transfer channels are included. It is clear for these cases that an additional mechanism must be invoked.

TABLE VI. Particle and hole states generated in one-neutron and one-proton pickup or stripping reactions on  $^{44}\text{Ca}$ . The spectroscopic factors for  $^{43}\text{Ca}$  and  $^{45}\text{Sc}$  are from Refs. 20 and 21, respectively.

$^{44}\text{Ca}$	$J^\pi$	$E$ (MeV)	$C^2S$
$^{43}\text{Ca}$	$\frac{7}{2}^-$	0.00	3.50
	$\frac{5}{2}^-$	0.37	0.27
	$\frac{3}{2}^-$	0.59	0.14
	$\frac{3}{2}^+$	0.99	2.50
$^{45}\text{Sc}$	$\frac{7}{2}^-$	0.00	0.71
	$\frac{3}{2}^+$	0.0124	0.53
	$\frac{3}{2}^-$	0.3761	0.14

TABLE VII. Particle and hole states generated in one-neutron and one-proton pickup or stripping reactions on  $^{48}\text{Ca}$ . The spectroscopic factors for  $^{47}\text{Ca}$  and  $^{49}\text{Sc}$  are from Refs. 22 and 23, respectively.

$^{48}\text{Ca}$	$J^\pi$	$E$ (MeV)	$C^2S$
$^{47}\text{Ca}$	$\frac{7}{2}^-$	0.00	6.70
	$\frac{3}{2}^+$	2.58	3.60
$^{49}\text{Sc}$	$\frac{7}{2}^-$	0.00	0.9788

The calculated proton and neutron transfer cross sections are shown in Fig. 3 together with the fusion data. The magnitudes of the transfer cross sections appear to be quite reasonable. They have a behavior with respect to the fusion data that is similar to that found in Ni+Ni reactions.<sup>24,25</sup> It is interesting to note that the proton transfer is dominant for each case. This reflects the very weak proton binding energy (1.08 MeV) in the  $^{39}\text{K}+^{41}\text{Sc}$  channel and the more favorable  $Q$  values in the  $^{40}\text{Ca}+^{44,48}\text{Ca}$  reactions (see Tables V–VII). The magnitudes of the cross sections also depend on the spectroscopic factors determined from light-ion transfer reactions. A comparison of the present calculated transfer cross sections with data would provide a direct test of the coupling strengths which have been used.

As one looks at the enhancement effects due to transfer alone shown by the dashed curves in Fig. 2 and the transfer cross sections in Fig. 3, one notes a nonintuitive feature in these results. The enhancement effect for  $^{40}\text{Ca}+^{48}\text{Ca}$  is about the same as for  $^{40}\text{Ca}+^{40}\text{Ca}$ , but the corresponding cross section is at least an order of magni-

tude larger. This can be understood by examining the details of the dominant single-proton transfer reaction in both cases. The relatively low transfer cross sections for  $^{40}\text{Ca}+^{40}\text{Ca}$  can be attributed to the unfavorable transfer  $Q$  value of  $-7.2$  MeV in this case. On the other hand, the effect of this channel on the fusion cross section is significant because the proton transfer coupling form factor is relatively large for  $^{40}\text{Ca}+^{40}\text{Ca}$ . In the barrier region it is about twice as large as in the  $^{40}\text{Ca}+^{48}\text{Ca}$  case. This results from the unusually weak proton binding energy in the  $^{39}\text{K}+^{41}\text{Sc}$  channel and from the  $\sqrt{2}$  weighting factor due to the symmetry of the stripping and pickup processes.

In the asymmetric Ca+Ca reactions, where the single-nucleon transfer cross sections are large, it can be expected that the elastic scattering cross sections will be affected by couplings to these channels. This would provide another means to check the transfer coupling strengths. However, measurements exist only for the symmetric case. In Fig. 4, the calculated elastic cross sections for  $^{40}\text{Ca}+^{40}\text{Ca}$  scattering are compared with the data at three energies.<sup>26</sup> The solid curves are obtained in the full calculation, while the dotted curves result when only the vibrational channels are included. For the two lowest energies, the comparison does not clearly demonstrate the effects of the transfer channels. However, in the highest-energy case, where the transfer cross section has increased to about 10 mb, the result obtained from the full calculation provides a much better fit to the data. This indicates that the couplings of the nucleon transfer channels are reasonably well determined for the case of  $^{40}\text{Ca}+^{40}\text{Ca}$ .

Since the inclusion of single-nucleon transfer and vibrational excitations has not resulted in a satisfactory explanation of the fusion data for  $^{40}\text{Ca}+^{44,48}\text{Ca}$ , it is in-

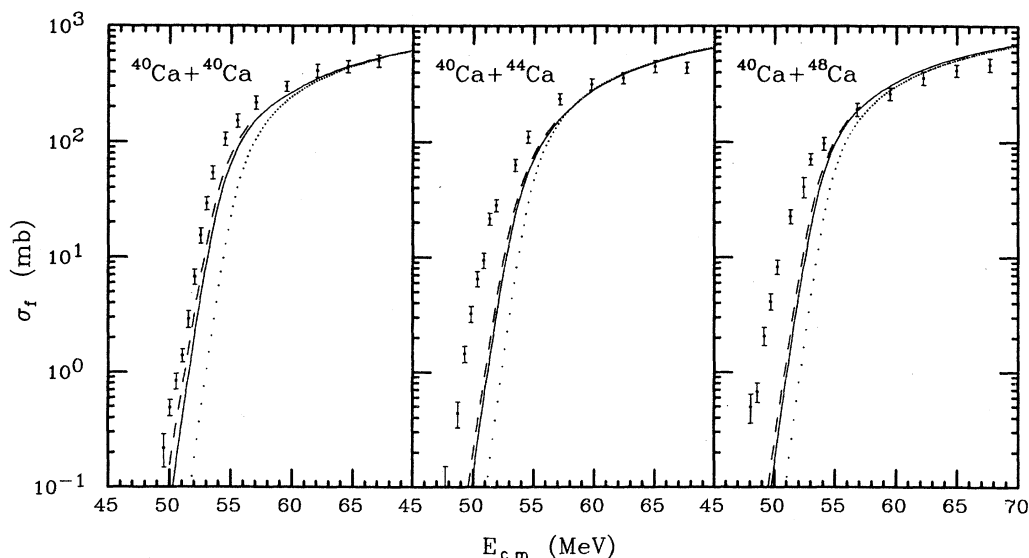


FIG. 1. The fusion cross sections including the effects of vibrational excitations. Shown are the no-coupling results (dotted line), results from first-order excitations (solid line), and results from second-order excitations (dashed line) compared to the data from Ref. 3.

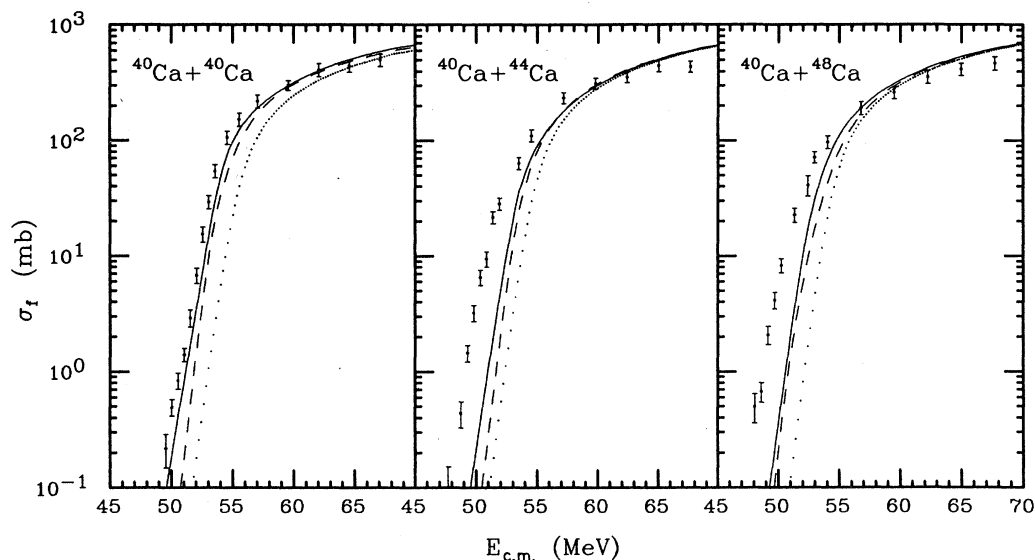


FIG. 2. Fusion cross sections resulting from including both vibrational and single-nucleon transfer channels. Shown are the no-coupling result (dotted line), the transfer only result (dashed line), and the result of the full calculation (solid line) compared to the data from Ref. 3.

interesting to speculate whether additional channels are contributing. In previous calculations for Ni+Ni and Si+Ni systems,<sup>1,2</sup> the role of two-nucleon transfer reactions has been estimated using the macroscopic approach of Ref. 27. As Table IV shows, there are two-nucleon transfer channels available for the asymmetric cases which have positive ground-state  $Q$  values that are favorable for fusion. To investigate this possibility, we have introduced an additional channel with a  $Q$  value of +1

MeV and a coupling proportional to the derivative of the ion-ion potential

$$V_t = -\sigma_t \frac{dU}{dr}. \quad (4.1)$$

A coupling strength of  $\sigma_t = 0.5$  fm was obtained by requiring a fit to the low-energy  $^{40}\text{Ca} + ^{48}\text{Ca}$  fusion data of the same quality as that already obtained for  $^{40}\text{Ca} + ^{40}\text{Ca}$  in Fig. 2.

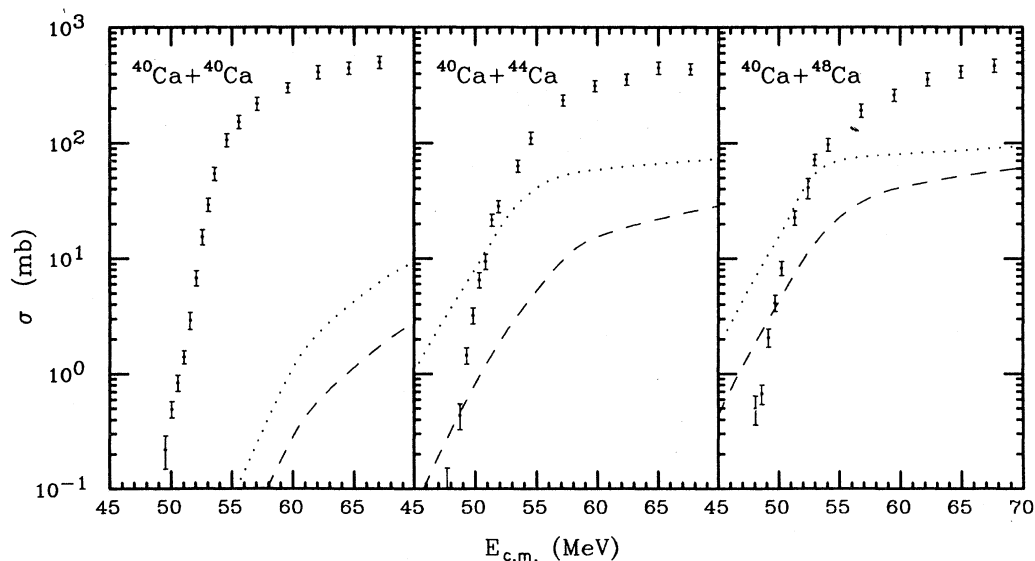


FIG. 3. Calculated single-nucleon transfer cross sections for the states included in Tables V-VII. The dotted and dashed lines indicate the proton and neutron transfer cross sections, respectively. The fusion data of Ref. 3 are also shown.

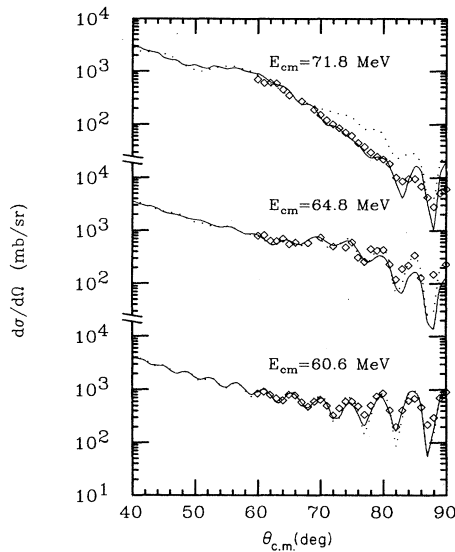


FIG. 4. The elastic scattering cross sections calculated for the  $^{40}\text{Ca} + ^{40}\text{Ca}$  reaction at the three indicated energies. The data are from Ref. 26. The solid curves are calculated with both vibrational and transfer channels included, while the dotted curves are obtained by including only the vibrational channels.

The results from this calculation are shown in Fig. 5(a). It is interesting to note that the extra coupling also reduces the cross section at the higher energies, bringing an overall agreement with the data. On the other hand, the required strength seems to be unreasonably large for a two-particle reaction. It is larger than the strengths of the collective vibrations in Table II. Also, the corresponding cross sections shown in Fig. 5(a) are comparable to those calculated for the single-nucleon transfer.

It should be kept in mind that additional negative  $Q$ -value channels could enhance the low-energy fusion. For instance, Table IV shows that the alpha transfer reaction is better matched for the asymmetric combinations. To illustrate this point we repeated the previous calculation using a  $Q$  value of  $-3$  MeV and a strength of  $\sigma_t = 0.9$  fm. The results<sup>28</sup> are shown in Fig. 5(b). The bigger mismatch in this case is offset by a larger strength so that the resulting cross section is about the same as in Fig. 5(a).

If in fact there are strongly coupled channels in addition to the vibrational excitations and the one-particle transfer reactions which we have included, they should have a significant influence on the elastic scattering cross section. This point is illustrated in Figs. 6(a) and 6(b) where the elastic scattering cross sections corresponding to the calculations in Figs. 5(a) and 5(b) are shown. The large modifications produced by the additional couplings indicate that measurements of the elastic scattering should be able to determine whether such strongly coupled channels are present.

## V. CONCLUSIONS

In this work we have used the coupled-channels approach to calculate the combined effects of vibrational

excitations and the most probable single-nucleon transfer reactions on the low-energy  $^{40}\text{Ca} + ^{40,44,48}\text{Ca}$  fusion reactions. For each case we have also presented the predicted transfer cross sections.

The results agree well with the  $^{40}\text{Ca} + ^{40}\text{Ca}$  fusion data. The calculations also compare favorably with the available elastic scattering measurements for this system. Thus the  $^{40}\text{Ca} + ^{40}\text{Ca}$  case provides a good reference point for determining the basic parameters of the ion-ion interaction.

The single-nucleon transfer cross sections are predicted to increase strongly in going from  $^{40}\text{Ca} + ^{40}\text{Ca}$  to the  $^{40}\text{Ca} + ^{44,48}\text{Ca}$  cases. It is interesting to note that the proton transfer strength is predicted to be larger than for the neutron transfer. Even though their strengths increase, the enhancement effects due to these transfer couplings when combined with those of the vibrational excitations

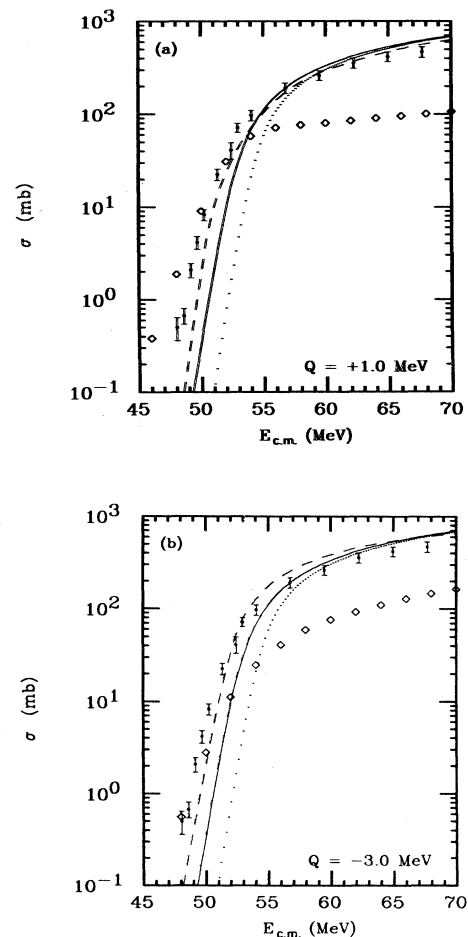


FIG. 5. The fusion cross sections obtained by including an additional channel in the calculation for the  $^{40}\text{Ca} + ^{48}\text{Ca}$  reaction (dashed line) using a strong vibrational type form factor of strength  $\sigma_t$ . The no-coupling result (dotted line) and the result without the effective channel (solid line) are also shown. The open points show the calculated cross sections for the extra channel. In part (a) the  $Q$  value is  $+1$  MeV and  $\sigma_t = 0.5$  fm while for part (b)  $Q = -3$  MeV and  $\sigma_t = 0.9$  fm.

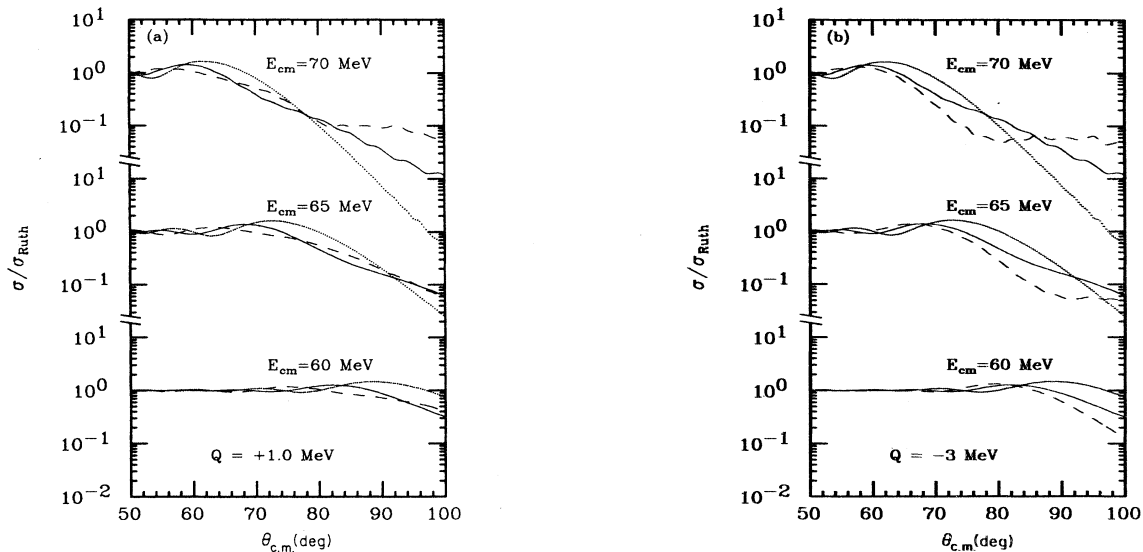


FIG. 6. The elastic scattering cross sections for  $^{40}\text{Ca} + ^{48}\text{Ca}$  corresponding to the two sets of calculations shown in Figs. 5(a) and 5(b).

are not sufficient to explain the low-energy  $^{40}\text{Ca} + ^{44,48}\text{Ca}$  fusion data. This discrepancy is judged to be particularly serious for the  $^{40}\text{Ca} + ^{48}\text{Ca}$  case since here both nuclei have simple closed-shell structures.

The options to explain this discrepancy appear to be rather restricted. Simply invoking a larger change in the ion-ion potential in going from  $^{40}\text{Ca} + ^{40}\text{Ca}$  to  $^{40}\text{Ca} + ^{48}\text{Ca}$  to improve the agreement with the low-energy fusion data would result in a severe overprediction of the higher-energy fusion cross section. The strengths of the vibrational excitations and single-nucleon transfers which we have included are constrained by other types of data. One can argue that there are single-particle transfers to higher-lying states which have not been included and their combined effect might significantly enhance the sub-barrier fusion. The relatively small effects we have obtained from the more favorable transfer reactions do not lend support to this argument. The low-energy fusion cross section can be increased specifically by introducing additional channels which couple directly to the initial state. Our estimates in the present case require a strong coupling resulting in a cross section which is comparable

to that of the single-nucleon transfer. This seems to be unreasonably large for two-particle transfer reactions alone. A combination of two-particle and alpha-particle transfer processes seems to be a more likely possibility.

It is necessary to have additional measurements for the  $^{40}\text{Ca} + ^{48}\text{Ca}$  system in order to better understand this problem. The elastic scattering cross section can provide useful information. It would further constrain the parameters of the ion-ion potential for the  $^{40}\text{Ca} + ^{48}\text{Ca}$  system. It should also reveal the presence, or absence, of any significant directly coupled channel not already included in the present calculations. Measurements of the single-nucleon transfer cross sections would directly check the conventional shell-model description which we have used, and measurements of the multiparticle transfer reactions would limit the present freedom one has to parametrize these processes.

This work was supported by the Department of Energy, Nuclear Physics Division, under Contract W-31-109-ENG-38.

- <sup>1</sup>H. Esbensen and S. Landowne, Nucl. Phys. **A492**, 473 (1989).
- <sup>2</sup>S. Landowne, S. C. Pieper, and F. Videbaek, Phys. Rev. C **35**, 597 (1987).
- <sup>3</sup>H. A. Aljuwair, R. J. Ledoux, M. Beckerman, S. B. Gazes, J. Wiggins, E. R. Cosman, R. R. Betts, S. Saini, and O. Hansen, Phys. Rev. C **30**, 1223 (1984).
- <sup>4</sup>S. Landowne, C. H. Dasso, R. A. Broglia, and G. Pollarolo, Phys. Rev. C **31**, 1047 (1985).
- <sup>5</sup>M. V. Andres, F. Catara, Ph. Chomaz, and E. G. Lanza, J. Phys. G **14**, 1331 (1988).
- <sup>6</sup>M. Baldo, A. Rapisarda, R. A. Broglia, and A. Winther, Nucl.

- Phys. **A490**, 471 (1988).
- <sup>7</sup>J. Gomez-Comacho and R. C. Johnson, J. Phys. G **12**, L235 (1986); **14**, 609 (1988); O. Tanimura, Phys. Rev. C **35**, 1600 (1987); H. Esbensen, S. Landowne, and C. Price, *ibid.* **36**, 1216 (1987).
- <sup>8</sup>G. W. Rawitscher, Nucl. Phys. **85**, 337 (1966).
- <sup>9</sup>J. M. Quesada, G. Pollarolo, R. A. Broglia, and A. Winther, Nucl. Phys. **A442**, 381 (1985).
- <sup>10</sup>A. Roberts, Nucl. Phys. **A196**, 465 (1972).
- <sup>11</sup>H. Esbensen and S. Landowne, Phys. Rev. C **35**, 2090 (1987).
- <sup>12</sup>R. A. Broglia and A. Winther, *Heavy Ion Reactions, Lecture*

- Notes (Benjamin, New York, 1981), Vol. 1.
- <sup>13</sup>G. D. Alkhazov, T. Bauer, R. Bertini, L. Bimbot, O. Bing, A. Boudard, G. Bruge, H. Catz, A. Chaumeaux, P. Couvert, J. M. Fontaine, F. Hibou, G. J. Igo, J. C. Lugol, and M. Matoba, Nucl. Phys. **A280**, 365 (1977).
- <sup>14</sup>K. E. Rehm, W. Henning, J. R. Erskine, D. G. Kovar, M. H. Macfarlane, S. C. Pieper, and M. Rhoades-Brown, Phys. Rev. C **25**, 1915 (1982).
- <sup>15</sup>H. Esbensen and F. Videback, Phys. Rev. C **40**, 126 (1989).
- <sup>16</sup>R. L. Kozub, Phys. Rev. **172**, 1078 (1968).
- <sup>17</sup>D. C. Kocher and W. Haeberli, Nucl. Phys. **A196**, 225 (1972).
- <sup>18</sup>J. C. Hiebert, E. Newman, and R. H. Bassel, Phys. Rev. **154**, 898 (1967).
- <sup>19</sup>D. H. Youngblood, R. L. Kozub, R. A. Kenefick, and J. C. Hiebert, Phys. Rev. C **2**, 477 (1970).
- <sup>20</sup>J. Rapaport, W. E. Dorenbusch, and T. A. Belote, Nucl. Phys. **A177**, 307 (1971).
- <sup>21</sup>J. J. Schwartz and W. P. Alford, Phys. Rev. **149**, 820 (1966).
- <sup>22</sup>P. Martin, M. Buenerd, Y. Dupont, and M. Chabre, Nucl. Phys. **A185**, 465 (1972).
- <sup>23</sup>R. M. Britton and D. L. Watson, Nucl. Phys. **A272**, 91 (1976).
- <sup>24</sup>J. Wiggins, R. Brooks, M. Beckerman, S. B. Gazes, L. Grodzins, A. P. Smith, S. G. Steadman, Y. Xiao, and F. Videbaek, Phys. Rev. C **31**, 1315 (1985).
- <sup>25</sup>K. E. Rehm, F. L. H. Wolfs, A. M. van den Berg, and W. Henning, Phys. Rev. Lett. **55**, 280 (1985).
- <sup>26</sup>M. Richter, W. Henning, H.-J. Körner, R. Müller, K. E. Rehm, H. P. Rother, H. Schaller, and H. Spieler, Nucl. Phys. **A278**, 163 (1977); H. Doubre, J. C. Jacmart, E. Plagnol, N. Poffe, M. Riou, and J. C. Roynette, Phys. Rev. C **15**, 693 (1977).
- <sup>27</sup>C. H. Dasso and G. Pollarolo, Phys. Lett. **B155**, 223 (1985); C. H. Dasso and A. Vitturi, *ibid.* **B 179**, 337 (1986).
- <sup>28</sup>A calculation similar to the one shown in Fig. 5(b) was made previously in Ref. 4. However, the implication in Ref. 4 that the cross section should be associated with single-nucleon transfer is not supported by the present results.